Journal of Quantitative Spectroscopy & Radiative Transfer 185 (2016) 70–78

Contents lists available at ScienceDirect

Journal of Quantitative Spectroscopy & Radiative Transfer

journal homepage: www.elsevier.com/locate/jqsrt

MCDHF calculations of isotope shifts of even-parity fine-structure levels in neutral osmium

P. Palmeri [a,*], P. Quinet [a,b], S. Bouazza [c]

[a] Physique Atomique et Astrophysique, Université de Mons – UMONS, B-7000 Mons, Belgium
[b] IPNAS, Université de Liège, B-4000 Liège, Belgium
[c] LISM, E.A. 4695 Université de Reims-Champagne-Ardenne, UFR SEN, BP 1039, F-51687 Reims Cedex 2, France

ARTICLE INFO

Article history:
Received 29 April 2016
Received in revised form
16 August 2016
Accepted 17 August 2016
Available online 24 August 2016

Keywords:
Isotope shift
Relativistic effects
Neutral osmium
Fine structure

ABSTRACT

Ab initio multiconfiguration Dirac–Hartree–Fock (MCDHF) calculations have been carried out in order to determine the isotope shifts of all the fine-structure levels belonging to the even-parity configurations $(5d+6s)^8$ in neutral osmium, Os I. The theoretical predictions have been compared to laser spectroscopy measurements available in the literature showing a good agreement between theory and experiment.

1. Introduction

The optical data of hyperfine structure (hfs) and/or isotope shifts (IS) for any element are used mainly to test atomic theory, to deduce nuclear moments and changes in the nuclear mean square charge radius and to give information on electron behaviour inside the nucleus. Thousands of high-resolution spectroscopic observations acquired over the last few decades have revealed that nearly all stars contain at least traces of elements heavier than the iron group. Osmium belongs to transition metals of the platinum group and then, as in the cases of its neighbour atoms in the Periodic Table, hfs and IS of many optical transitions in atomic osmium have been studied; the early measurements were initiated by Murakawa and Suwa to determine the nuclear spin value of ^{189}Os [1]. Some years later Guthöhrlein et al. [2] evaluated successfully the nuclear spin of ^{187}Os. These two teams had *recourse* to classical Doppler-limited spectroscopy using hollow-cathode light sources with isotopically enriched osmium samples and a Fabry–Perot interferometer. The IS in 5 lines of the osmium spectrum, involving transitions of the type $5d^66s6p–5d^66s^2$ were measured with similar experimental set-up [3]. More recently IS in the arc spectrum of osmium was studied in 10 lines for the highly enriched isotopes ^{188}Os and ^{192}Os and in 2 lines for natural ^{190}Os [4] by means of photoelectric recording Fabry–Perot spectrometer with digital data processing.

During these two last decades real accuracy improvements of experimental measurements were observed since high-resolution Doppler-free laser techniques have been employed giving very good resolution of the individual isotopic and hyperfine components. For example laser induced fluorescence spectroscopy has been applied to measure IS and hfs of Os I spectral lines in the visible range [5]. We have also to mention that other sophisticated measurements of the isotope shifts of the stable $^{184,186–190,192}$Os isotopes have been made using the crossed-beams technique in Manchester [6]: atomic beams of Os were produced by laser ablation of pills of compressed natural Os powder whose diameter and thickness were 5 mm and 3 mm. IS for the stable $^{184–192}$Os and ^{187,189}Os

* Corresponding author.
E-mail address: patrick.palmeri@umons.ac.be (P. Palmeri).

http://dx.doi.org/10.1016/j.jqsrt.2016.08.014
0022-4073/

isotopes were measured [7], relative to ^{192}Os using two Doppler-free techniques. The hyperfine parameters of ^{189}Os, essential for the calibration of the radioactive isotopes have been extracted. As regard theoretical investigations Gluck et al. [8], Bauche [9], Aufmuth et al. [4] applied parametric analyses to the interpretation of the atomic isotope shift in intermediate coupling and configuration interaction. To this aim they took advantage of fine structure studies of van Kleef and Klinkenberg [10] which gave the eigenvector values of 155 Os I levels among 263 which were known at that moment. Furthermore we have to point out that sometimes they *had recourse* to *ab initio* calculations for comparison with experimental data. They used the non-relativistic Hartree–Fock method. In opposite we propose in the present work to use the relativistic Dirac–Hartree–Fock method to analyse experimental data of Os I isotope shift found in the literature without any theoretical background [5].

In this study, it is preferable, as it was done successfully in the case of singly ionised lead [11], to use the latter method because one can consider osmium as a heavy element since it lies near lead in Mendeleev Table. In this case relativistic effects are not negligible, particularly regarding the field shift (also referred to as the volume shift) due to contributions of $np_{1/2}$, not existing in simple Hartree–Fock scheme where only s-electrons are considered as contact (with nucleus) electrons and where $p_{1/2}$ and $p_{3/2}$ electrons are not distinguished.

2. MCDHF calculations

The multiconfiguration Dirac–Hartree–Fock (MCDHF) calculations have been carried out using the GRASP2K atomic structure package version 1_1 [12] along with its isotope shift module RIS3 [13]. A description of the method is given below.

2.1. Isotope shifts

The frequency spectral transition ν_{ul} connecting an upper level E_u to a lower level E_l is given by

$$\nu_{ul} = \frac{E_u - E_l}{h} \tag{1}$$

It differs from an isotope of mass M to another of mass M' by

$$\delta\nu_{ul}^{M,M'} \equiv \nu_{ul}^{M} - \nu_{ul}^{M'} = \frac{\delta E_u^{M,M'} - \delta E_l^{M,M'}}{h} \tag{2}$$

with

$$\delta E_i^{M,M'} \equiv E_i^{M} - E_i^{M'} (i = u, l) \tag{3}$$

and can be parameterised (with $M > M'$) [13] as

$$\delta\nu_{ul}^{M,M'} = \left(\frac{M' - M}{MM'}\right)\Delta\tilde{K}_{ul} + F_{ul}\delta\langle r^2\rangle^{M,M'} \tag{4}$$

where $\Delta\tilde{K}_{ul} = \tilde{K}_u - \tilde{K}_l$ refers to the mass-shift electronic parameter, $F_{ul} = F_u - F_l$ is the field-shift electronic factor and $\delta\langle r^2\rangle^{M,M'} \equiv \langle r^2\rangle^{M} - \langle r^2\rangle^{M'}$ is the nuclear mean-square radius difference between the two isotopes.

The relativistic mass-shift electronic parameter $\tilde{K}_{RMS}$ for a level is related to the expectation value of the relativistic recoil Hamiltonian, H_{RMS},

$$\tilde{K}_{RMS} = \frac{M}{h}\langle\Psi|H_{RMS}|\Psi\rangle \tag{5}$$

or, in energy unit,

$$K_{RMS} = h\,\tilde{K}_{RMS} \tag{6}$$

where H_{RMS} can be split into a one-body, the relativistic normal mass-shift (RNMS), operator and a two-body, the relativistic specific mass-shift (RSMS), operator [14–16]

$$H_{RMS} = H_{RNMS} + H_{RSMS} \tag{7}$$

$$H_{RNMS} = \frac{1}{2M}\sum_i \left[p_i^2 - \frac{\alpha Z}{r_i}\left[\vec{\alpha}_i + \frac{(\vec{\alpha}_i\cdot\vec{r}_i)\vec{r}_i}{r_i^2}\right]\cdot\vec{p}_i\right] \tag{8}$$

$$H_{RSMS} = \frac{1}{2M}\sum_{i\neq j}\left[\vec{p}_i\cdot\vec{p}_j - \frac{\alpha Z}{r_i}\left[\vec{\alpha}_i + \frac{(\vec{\alpha}_i\cdot\vec{r}_i)\vec{r}_i}{r_i^2}\right]\cdot\vec{p}_j\right] \tag{9}$$

The field-shift (FS) electronic factor F_{ul} is related to the change of the electronic total probability density, $\Delta|\Psi(\vec{0})|_{ul}^2 \equiv \rho_u^e(\vec{0}) - \rho_l^e(\vec{0})$, at the origin between the two levels involved in the transition [13]

$$F_{ul} = \frac{Z}{3\hbar}\left(\frac{e^2}{4\pi\epsilon_0}\right)\Delta\left|\Psi\left(\vec{0}\right)\right|_{ul}^2 \tag{10}$$

The total probability density at the origin is defined for a level by

$$\rho^e(\vec{0}) \equiv \left\langle\Psi\left|\sum_i\delta(\vec{r}_i)\right|\Psi\right\rangle \tag{11}$$

2.2. The MCDHF approach

In the MCDHF method [12], the atomic state function (ASF), Ψ, appearing in Eqs. (5) and (11) is represented by a linear combination of configuration state functions (CSFs), Φ, with the same parity, Π, total angular momentum and total magnetic quantum numbers, J and M_J, as

$$\Psi(\Pi\, J\, M_J) = \sum_i c_i\Phi(\gamma_i\Pi\, J\, M_J) \tag{12}$$

where c_i is the mixing coefficient, γ_i stands for all the other quantum numbers needed to specify the CSF which is in turn linear combinations of Slater determinants built from monoelectronic spin–orbitals, $\phi_{n\kappa m}$, of the form:

$$\phi_{n\kappa m}(r,\theta,\varphi) = \frac{1}{r}\begin{pmatrix} P_{n\kappa}(r)\chi_{\kappa m}(\theta,\varphi) \\ iQ_{n\kappa}(r)\chi_{-\kappa m}(\theta,\varphi)\end{pmatrix}, \tag{13}$$

where $P_{n\kappa}(r)$ and $Q_{n\kappa}(r)$ are, respectively, the large and the small component of the radial wave functions, and the angular functions $\chi_{\kappa m}(\theta,\varphi)$ are the spinor spherical harmonics [17]. The quantum number κ is given by:

$$\kappa = \pm\left(j + \frac{1}{2}\right), \tag{14}$$

where j is the electron total angular momentum. The sign before the parentheses in Eq. (14) corresponds to the coupling relation between the electron orbital momentum, ℓ,

and its spin, i.e.,

$$\ell = j \pm \frac{1}{2}. \tag{15}$$

The radial functions $P_{n\kappa}(r)$ and $Q_{n\kappa}(r)$ are numerically represented on a logarithmic grid and are required to be orthonormal within each κ symmetry. In the MCDHF variational procedure, the radial functions and the expansion coefficients c_i are optimised to self-consistency.

A spherical model, here a Fermi nucleus, has been chosen for the nuclear charge distribution as required for the first-order perturbation approximation of the field shift given in Eqs. (4 and (10) to be valid.

$$\rho(r) = \frac{\rho_0}{1 + e^{(r-c)/a}} \tag{16}$$

where ρ_0 is a normalisation constant, c the half-density of the nuclear charge distribution and $a = t/(4\ln(3))$ is related to the nuclear surface thickness t, with c computed according to [18] and $t = 2.30$ fm.

2.3. Computational strategy

The restricted active space (RAS) [19] method has been considered for building the MCDHF multiconfiguration expansions. The latter are produced by exciting the electrons from the reference configurations to a given set of spin–orbitals. The rules adopted for generating the configuration space differ according to the correlation model used. Within a given correlation model, the active set of spin–orbitals spanning the configuration space is increased to monitor the convergence of the total energies and the isotope shifts.

Our calculations have been focused on the isotope shift electronic parameters of the levels of the lowest excited even-parity interacting configuration $5d^6 6s^2 + 5d^7 6s + 5d^8$ in Os I ($Z = 76$). The reference isotope has been chosen to be the most abundant stable isotope with mass number $A = 192$ [20]. These calculations have been carried out in six steps:

- *Step* 1: The core orbitals, i.e. 1s to 5p, along with the 5d and 6s orbitals, have been optimised. All the 81 CSFs belonging the even-parity interacting configurations $5d^6 6s^2 + 5d^7 6s + 5d^8$ with symmetries $J = 0 - 6$ were retained in the configuration space. The energy functional was built within the framework of the average level (AL) option [17]. This option is most suitable for cases where all the eigenvalues of the hamiltonian are optimised *at once*. This is the case here as we want to obtain all the 81 ASFs belonging to $(5d^6 6s^2 + 5d^7 6s + 5d^8)$ $J = 0 - 6$.
- *Step* 2: The configuration space was increased to 16,619 CSFs by considering all the single and double electron excitations to the 5f and 5g orbitals from the active orbitals 5d and 6s of the multi-reference configurations $(5d^6 6s^2 + 5d^7 6s + 5d^8)$ $J = 1 - 6$. The 5f and 5g orbitals have been optimised, fixing all the others to the values of Step 1 using an energy functional built from the lowest 81 ASFs within the framework of the extended optimal level (EOL) option [17].
- *Steps* 3–5: The configuration space has been extended to 111,701, 305,051 and 594,075 CSFs, respectively, using the same optimisation procedure as described in Step 2 but considering single and double *excitations* to the {6p, 6d, 6f, 6g}, {6p, 6d, 6f, 6g, 7s, 7p, 7d, 7f, 7g} and {6p ,6d ,6f ,6g , 7s ,7p ,7d, 7f, 7g, 8s, 8p, 8d, 8f, 8g} orbital sets successively.
- *Step* 6: The core–valence and core–core correlations have been considered where a relativistic configuration interaction (RCI) calculation [12] has been carried out. In particular, a Dirac–Coulomb–Breit Hamiltonian has been diagonalised using the 594,075 CSFs and orbitals of the previous step along with 1 526 core-excited CSFs generated from single and double electron *excitations* of the {4f, 5s, 5p} core orbitals to the {5d, 6s} valence orbitals of the same multi-reference configurations as in Step 2.

3. Results and discussion

In Table 1, the electronic isotope shift parameters are presented for all the known even-parity levels belonging to the configurations $(5d+6s)^8$ along with their corresponding calculated and experimental energies taken from [8]. The average deviation of our *ab initio* MCDHF level energies with respect to the experimental values of Gluck et al. [8] is 564 cm^{-1}. The latter is 2% of the investigated experimental energy range, i.e. 31,765 cm^{-1}, which represents a fair theory-experiment agreement considering the complexity of the atomic structure of this heavy neutral element. Concerning the isotope shift parameters shown in this table, one can see the dominance of the normal mass shift contribution over the specific mass shift by a factor of 3 having opposite signs.

What is accessible to experiment is the differences between values corresponding to two fine-structure levels. These differences with respect to the ground level are presented in Table 2. They range from a few hundreds to a few thousands GHz u for the RNMS parameter, from a few tens to a few thousands GHz u for the RSMS parameter and from a few tenths to a few tens GHz/fm^2 for the FS factor. For most of the levels, the RNMS and RSMS parameters have opposite signs and almost cancel each other given rise to a low absolute value for the total mass shift parameter (shown in the sixth column). Also, when one compares the level energies given in the first column to the RNMS parameters of fourth column, the so called 'scaling law', where the NMS parameter is *proportional* to the transition energy in the non-relativistic limit [21,22], is clearly breakdown for this high-Z element ($Z = 76$). Indeed, higher-order relativistic contributions, $\Delta\tilde{K}^{(2+3)}_{RNMS}$, (related to the last two terms in αZ of the recoil hamiltonian operator presented in Eq. (8)) to the total RNMS parameter are shown in Table 3. One can see that these terms are far from being negligible. Moreover, even the term $\Delta\tilde{K}^{(1)}_{RNMS}$ related to the recoil operator $\frac{1}{2M}\sum_i p_i^2$ is not linear with respect to the level energy in agreement with the statement that, as long as Dirac electronic wave functions are used, one cannot expect that the operator $\frac{1}{2M}\sum_i p_i^2$ leads to

the scaling law [21,23]. The same kind of comparisons is made for the SMS in Table 4 where the higher-order relativistic contributions are found to be important as well for the majority of the levels.

Concerning the FS factors listed in Table 2, which are *proportional* to a change of the electron probability density at the nucleus with respect to the ground state ($5d^6 6s^2\ ^5D_4$) in this case, one can notice the important differences between, for instance, the values for the $5d^6 6s^2\ ^5D_{0,1,2,3}$ levels and those for the $5d^7 6s\ ^5F_{1,2,3,4,5}$ levels. These levels belong almost entirely to respectively the $5d^6 6s^2$ and $5d^7 6s$ configurations with admixtures $\gtrsim 90\%$ (see, Table VI in Ref. [5]), and therefore these differences can be related to the number of electrons in the 6s orbitals. All the levels labelled as belonging to the $5d^8$ configuration are unfortunately strongly mixed with the other configurations of the complex $(5d+6s)^8$ [5].

Table 1

Experimental level energies, E_{exp}, MCDHF level energies, E_{cal}, level normal mass shift parameter, $\tilde{K}_{RNMS}$, level specific mass shift parameter, $\tilde{K}_{RSMS}$, and level field-shift electronic factor, F, for all known even-parity levels belonging to the $(5d+6s)^8$ configurations in Os I.

E_{exp}[a] (cm^{-1})	E_{cal} (cm^{-1})	ΔE[b] (cm^{-1})	J	Designation[c]	$\tilde{K}_{RNMS}$ (GHz u)	$\tilde{K}_{RSMS}$ (GHz u)	F (GHz fm^{-2})
0.00	0	0	4	$5d^6 6s^2\ ^5D$	5.8904685(+7)	−1.9057176(+7)	6.2520113(+5)
2740.49	2254	−487	2	$5d^6 6s^2 {}^5D$	5.8905060(+7)	−1.9057356(+7)	6.2519866(+5)
4159.32	3930	−229	3	$5d^6 6s^2 {}^5D$	5.8904129(+7)	−1.9056962(+7)	6.2520158(+5)
5143.92	4718	−426	5	$5d^7(^4F)6s\,^5F$	5.8908742(+7)	−1.9060636(+7)	6.2516952(+5)
5766.14	5206	−560	1	$5d^6 6s^2 {}^5D$	5.8904172(+7)	−1.9056962(+7)	6.2520094(+5)
6092.79	5461	−631	0	$5d^6 6s^2 {}^5D$	5.8904133(+7)	−1.9056872(+7)	6.2520128(+5)
8742.83	8143	−599	4	$5d^7(^4F)6s\,^5F$	5.8908266(+7)	−1.9060403(+7)	6.2517009(+5)
10,165.98	9478	−688	2	$5d^6 6s^2 {}^5D$	5.8905237(+7)	−1.9057903(+7)	6.2519174(+5)
11,030.58	11,212	181	4	$5d^6 6s^2\ ^3G$	5.8905057(+7)	−1.9057769(+7)	6.2519376(+5)
11,378.00	10,454	−924	3	$5d^7(^4F)\ 6s\,^5F$	5.8908071(+7)	−1.9060297(+7)	6.2516986(+5)
12,774.38	11,820	−954	2	$5d^7(^4F)\ 6s\,^5F$	5.8907800(+7)	−1.9060095(+7)	6.2517106(+5)
13,020.07	12,109	−911	1	$5d^7(^4F)\ 6s\,^5F$	5.8907822(+7)	−1.9060050(+7)	6.2517117(+5)
13,364.83	12,938	−427	2	$5d^6 6s^2\ ^3F$	5.8905216(+7)	−1.9057835(+7)	6.2519226(+5)
14,091.37	13,867	−225	3	$5d^6 6s^2\ ^3F$	5.8905616(+7)	−1.9058263(+7)	6.2518789(+5)
14,338.99	15,306	967	5	$5d^6 6s^2\ ^3G$	5.8904375(+7)	−1.9057430(+7)	6.2519731(+5)
14848.05	15,325	477	4	$5d^7(^4F)\ 6s\ ^3F$	5.8906677(+7)	−1.9059175(+7)	6.2517940(+5)
14,852.33	16,293	1440	6	$5d^6 6s^2\ ^3H$	5.8903866(+7)	−1.9057245(+7)	6.2520045(+5)
15,222.57	14,893	−329	2	$5d^7(^4P)\ 6s\,^5P$	5.8907237(+7)	−1.9059231(+7)	6.2517607(+5)
15,390.76	14,961	−430	3	$5d^7(^4P)\ 6s\,^5P$	5.8907374(+7)	−1.9059435(+7)	6.2517472(+5)
16,212.41	15,299	−913	1	$5d^7(^4P)\ 6s\,^5P$	5.8907240(+7)	−1.9059472(+7)	6.2517484(+5)
17,667.34	17,270	−398	1	$5d^6 6s^2\ ^3P$	5.8905392(+7)	−1.9058014(+7)	6.2518744(+5)
18,301.40	16,937	−1365	0	$5d^7\ (^2P)\ 6s\ ^3P$	5.8904418(+7)	−1.9057195(+7)	6.2519410(+5)
18,417.12	18,856	439	5	$5d^7\ (^2G)\ 6s\ ^3G$	5.8906064(+7)	−1.9059001(+7)	6.2518232(+5)
18,901.94	18,699	−203	3	$5d^6 6s^2\ ^3D$	5.8906049(+7)	−1.9058519(+7)	6.2518239(+5)
19,048.91	18,966	−83	0	$5d^6 6s^2\ ^3P$	5.8906183(+7)	−1.9058500(+7)	6.2518258(+5)
19,108.87	19,270	161	4	$5d^6 6s^2\ ^3G$	5.8905757(+7)	−1.9058655(+7)	6.2518407(+5)
19,410.66	19,068	−343	2	$5d^6 6s^2\ ^3D$	5.8905075(+7)	−1.9057825(+7)	6.2518983(+5)
19,893.07	20,292	399	4	$5d^6 6s^2\ ^3H$	5.8904923(+7)	−1.9058002(+7)	6.2518923(+5)
21,033.45	20,425	−609	1	$5d^6 6s^2\ ^3D$	5.8906555(+7)	−1.9058946(+7)	6.2517704(+5)
21,123.66	20,954	−170	3	$5d^6 6s^2\ ^3G$	5.8904959(+7)	−1.9058017(+7)	6.2518875(+5)
21,303.36	20,928	−375	2	$5d^6 6s^2\ ^3D$	5.8905522(+7)	−1.9058094(+7)	6.2518549(+5)
22,563.65	21,817	−747	1	$5d^7(^4P)\ 6s\,^5P$	5.8905335(+7)	−1.9057994(+7)	6.2518572(+5)
23,317.60	22,315	−1003	2	$5d^7\ (^2P)\ 6s\ ^3P$	5.8907002(+7)	−1.9059260(+7)	6.2517274(+5)
23,322.66	23,790	467	4	$5d^7\ (^2G)\ 6s\ ^1G$	5.8906778(+7)	−1.9059457(+7)	6.2517412(+5)
23,984.58	23,997	12	3	$5d^7(^4F)\ 6s\ ^3F$	5.8906103(+7)	−1.9058793(+7)	6.2517816(+5)
24,222.97	25,285	1062	6	$5d^7\ (^2H)\ 6s\ ^3H$	5.8907147(+7)	−1.9059965(+7)	6.2517158(+5)
24,291.97	25,082	790	5	$5d^6 6s^2\ ^3G$	5.8904389(+7)	−1.9057573(+7)	6.2519024(+5)
25,069.71	24,637	−433	2	$5d^7(^4F)\ 6s\ ^3F$	5.8907089(+7)	−1.9059608(+7)	6.2516923(+5)
25,593.96	25,922	329	3	$5d^7\ (^2G)\ 6s\ ^3G$	5.8905526(+7)	−1.9058224(+7)	6.2518314(+5)
25,601.55	26,359	757	4	$5d^8\ ^3F$	5.8905526(+7)	−1.9058489(+7)	6.2518123(+5)
26,200.42	26,760	560	4	$5d^7\ (^2G)\ 6s\ ^3G$	5.8907905(+7)	−1.9060414(+7)	6.2516492(+5)
26,416.35	28,147	1730	6	$5d^6 6s^2\ ^1I$	5.8902902(+7)	−1.9056889(+7)	6.2520072(+5)
26,783.05	27,618	835	5	$5d^7\ (^2H)\ 6s\ ^3H$	5.8907150(+7)	−1.9060003(+7)	6.2516941(+5)
27,350.96	27,737	386	3	$5d^6 6s^2\ ^3G$	5.8905266(+7)	−1.9057743(+7)	6.2518321(+5)
28,139.52	27,870	−270	3	$5d^7\ (^2D)\ 6s\ ^3D$	5.8905226(+7)	−1.9058125(+7)	6.2518347(+5)
28,411.95	28,127	−285	2	$5d^7(^4P)\ 6s\ ^3P$	5.8906158(+7)	−1.9058513(+7)	6.2517536(+5)
29,394.30	29,935	540	4	$5d^6 6s^2\ ^1G$	5.8905988(+7)	−1.9058922(+7)	6.2517573(+5)
30,056.79	30,751	695	2	$5d^8\ ^3F$	5.8906739(+7)	−1.9059220(+7)	6.2517087(+5)
31,765.12	32,173	408	3	$5d^8\ ^3F$	5.8907244(+7)	−1.9059857(+7)	6.2516511(+5)

[a] Gluck et al. [8].
[b] $\Delta E = E_{exp} - E_{cal}$.
[c] Kröger et al. [5].

Table 2

MCDHF level normal mass shift parameter, $\Delta\tilde{K}_{RNMS}$, specific mass shift parameter, $\Delta\tilde{K}_{RSMS}$, total mass shift parameter , $\Delta\tilde{K}^{Tot}_{RMS}$ and field-shift electronic factor, F_{ul}, with respect to the ground level for all known even-parity levels belonging to the $(5d+6s)^8$ configurations in Os I.

E_{exp}[a] (cm^{-1})	J	Designation[b]	$\Delta\tilde{K}_{RNMS}$ (GHz u)	$\Delta\tilde{K}_{RSMS}$ (GHz u)	$\Delta\tilde{K}^{Tot}_{RMS}$ (GHz u)	F_{ul} (GHz/fm^2)
0.00	4	$5d^66s^2\,^5D$	0	0	0	0.00
2740.49	2	$5d^66s^2\,^5D$	374	−180	193	−2.47
4159.32	3	$5d^66s^2\,^5D$	−557	215	−342	0.45
5143.92	5	$5d^7(^4F)\,6s\,^5F$	4058	−3460	598	−31.60
5766.14	1	$5d^66s^2\,^5D$	−512	214	−298	−0.19
6092.79	0	$5d^66s^2\,^5D$	−553	304	−250	0.15
8742.83	4	$5d^7(^4F)\,6s\,^5F$	3582	−3227	355	−31.04
10,65.98	2	$5d^66s^2\,^5D$	552	−727	−175	−9.39
11,030.58	4	$5d^66s^2\,^3G$	373	−593	−220	−7.37
11,378.00	3	$5d^7(^4F)\,6s\,^5F$	3385	−3121	264	−31.27
12,774.38	2	$5d^7(^4F)\,6s\,^5F$	3116	−2919	198	−30.07
13,020.07	1	$5d^7(^4F)\,6s\,^5F$	3137	−2874	263	−29.96
13,364.83	2	$5d^66s^2\,^3F$	531	−659	−129	−8.86
14,091.37	3	$5d^66s^2\,^3F$	930	−1087	−157	−13.24
14,338.99	5	$5d^66s^2\,^3G$	−311	−254	−566	−3.81
14,848.05	4	$5d^7(^4F)\,6s\,^3F$	1993	−1999	−6	−21.73
14,852.33	6	$5d^66s^2\,^3H$	−819	−68	−887	−0.67
15,222.57	2	$5d^7(^4P)\,6s^5P$	2550	−2055	495	−25.06
15,390.76	3	$5d^7(^4P)\,6s^5P$	2688	−2259	429	−26.40
16,212.41	1	$5d^7(^4P)\,6s^5P$	2555	−2296	259	−26.29
17,667.34	1	$5d^66s^2\,^3P$	708	−838	−130	−13.69
18,301.40	0	$5d^7\,(^2P)\,6s\,^3P$	−267	−19	−286	−7.03
18,417.12	5	$5d^7\,(^2G)\,6s\,^3G$	1378	−1824	−447	−18.81
18,901.94	3	$5d^66s^2\,^3D$	1364	−1343	21	−18.74
19,048.91	0	$5d^66s^2\,^3P$	1499	−1323	176	−18.55
19,108.87	4	$5d^66s^2\,^3G$	1072	−1479	−407	−17.05
19,410.66	2	$5d^66s^2\,^3D$	389	−649	−260	−11.29
19,893.07	4	$5d^66s^2\,^3H$	238	−826	−587	−11.89
21,033.45	1	$5d^66s^2\,^3D$	1871	−1769	102	−24.09
21,123.66	3	$5d^66s^2\,^3G$	274	−841	−567	−12.38
21,303.36	2	$5d^66s^2\,^3D$	837	−917	−81	−15.63
22,563.65	1	$5d^7(^4P)\,6s^5P$	648	−818	−170	−15.41
23,317.60	2	$5d^7(^2P)\,6s\,^3P$	2318	−2084	234	−28.39
23,322.66	4	$5d^7(^2G)\,6s\,^1G$	2093	−2281	−187	−27.00
23,984.58	3	$5d^7(^4F)\,6s\,^3F$	1419	−1617	−198	−22.96
24,222.97	6	$5d^7\,(^2H)\,6s\,^3H$	2461	−2789	−329	−29.55
24,291.97	5	$5d^66s^2\,^3G$	−297	−397	−694	−10.88
25,069.71	2	$5d^7(^4F)\,6s\,^3F$	2405	−2432	−27	−31.90
25,593.96	3	$5d^7\,(^2G)\,6s\,^3G$	841	−1048	−207	−17.99
25,601.55	4	$5d^8\,^3F$	840	−1313	−472	−19.90
26,200.42	4	$5d^7\,(^2G)\,6s\,^3G$	3219	−3238	−19	−36.20
26,416.35	6	$5d^66s^2\,^1I$	−1784	288	−1497	−0.41
26,783.05	5	$5d^7\,(^2H)\,6s\,^3H$	2465	−2827	−362	−31.72
27,350.96	3	$5d^66s^2\,^3G$	581	−567	15	−17.91
28,139.52	3	$5d^7\,(^2D)\,6s\,^3D$	540	−949	−409	−17.65
28,411.95	2	$5d^7(^4P)\,6s\,^3P$	1473	−1337	137	−25.77
29,394.30	4	$5d^66s^2\,^1G$	1304	−1746	−442	−25.39
30,056.79	2	$5d^8\,^3F$	2055	−2044	11	−30.26
31,765.12	3	$5d^8\,^3F$	2560	−2680	−121	−36.02

[a] Gluck et al. [8].
[b] Kröger et al. [5].

Illustrations of the convergence of our isotope shift parameter values with respect to those of the ground level are given in Fig. 1 for the $5d^66s^2\,^5D_2$ level and in Fig. 2 for the $5d^76s\,^5F_5$ level where each parameter is plotted against the MCDHF calculation step described in the previous section. Sensitivity of these parameters to correlation can be appreciated from these figures. One can also notice that convergence is achieved in the last three steps for all parameters if we except the FS factor of the $5d^76s\,^5F_5$ level where it oscillates around ~ -32 GHz/fm^2 with an amplitude of ~ 2 GHz/fm^2 (i.e. $a \sim 10\%$ amplitude).

The electronic parameters given in Table 1 can be used for any pair of isotopes of neutral osmium to determine the isotope shifts.

Kröger et al. [5] determined experimentally ^{192}Os I residual level isotope shifts, i.e. the isotope shifts minus the normal mass shift contributions, with respect to the ground level of the isotope ^{190}Os I. In order to determine

Table 3
Higher-order relativistic contributions to the level normal mass shift (NMS) parameter with respect to the ground level for all known even-parity levels belonging to the $(5d+6s)^8$ configurations in Os I. $\Delta\tilde{K}^{(1)}_{NMS}$ and $\Delta\tilde{K}^{(2+3)}_{NMS}$ are respectively related to the first term and to the sum of the second and third terms of the recoil NMS Hamiltonian (see Eq. (8)). $\Delta\tilde{K}^{(1+2+3)}_{NMS}$ is the total NMS parameter.

E_{exp}[a] (cm^{-1})	J	Designation[b]	$\Delta\tilde{K}^{(1)}_{NMS}$ (GHz u)	$\Delta\tilde{K}^{(2+3)}_{NMS}$ (GHz u)	$\Delta\tilde{K}^{(1+2+3)}_{NMS}$ (GHz u)
0.00	4	$5d^6 6s^2\,^5D$	0	0	0
2740.49	2	$5d^6 6s^2\,^5D$	273	101	374
4159.32	3	$5d^6 6s^2\,^5D$	−793	236	−557
5143.92	5	$5d^7(^4F)\,6s\,^5F$	2466	1591	4058
5766.14	1	$5d^6 6s^2\,^5D$	−795	282	−512
6092.79	0	$5d^6 6s^2\,^5D$	−788	235	−553
8742.83	4	$5d^7(^4F)\,6s\,^5F$	1849	1733	3582
10,165.98	2	$5d^6 6s^2\,^5D$	−271	824	552
11,030.58	4	$5d^6 6s^2\,^3G$	−142	514	373
11,378.00	3	$5d^7(^4F)\,6s\,^5F$	1531	1854	3385
12,774.38	2	$5d^7(^4F)\,6s\,^5F$	1281	1835	3116
13,020.07	1	$5d^7(^4F)\,6s\,^5F$	1345	1792	3137
13,364.83	2	$5d^6 6s^2\,^3F$	−133	664	531
14,091.37	3	$5d^6 6s^2\,^3F$	9	921	930
14,338.99	5	$5d^6 6s^2\,^3G$	−702	390	−311
14,848.05	4	$5d^7(^4F)\,6s\,^3F$	826	1167	1993
14,852.33	6	$5d^6 6s^2\,^3H$	−1063	245	−819
15,222.57	2	$5d^7(^4P)\,6s\,^5P$	1127	1423	2550
15,390.76	3	$5d^7(^4P)\,6s\,^5P$	1136	1552	2688
16,212.41	1	$5d^7(^4P)\,6s\,^5P$	871	1684	2555
17,667.34	1	$5d^6 6s^2\,^3P$	−379	1087	708
18,301.40	0	$5d^7\,(^2P)\,6s\,^3P$	−1114	847	−267
18,417.12	5	$5d^7\,(^2G)\,6s\,^3G$	132	1245	1378
18,901.94	3	$5d^6 6s^2\,^3D$	143	1221	1364
19,048.91	0	$5d^6 6s^2\,^3P$	303	1196	1499
19,108.87	4	$5d^6 6s^2\,^3G$	−131	1203	1072
19,410.66	2	$5d^6 6s^2\,^3D$	−565	955	389
19,893.07	4	$5d^6 6s^2\,^3H$	−732	971	238
21,033.45	1	$5d^6 6s^2\,^3D$	256	1615	1871
21,123.66	3	$5d^6 6s^2\,^3G$	−834	1108	274
21,303.36	2	$5d^6 6s^2\,^3D$	−341	1178	837
22,563.65	1	$5d^7(^4P)\,6s\,^5P$	−638	1286	648
23,317.60	2	$5d^7\,(^2P)\,6s\,^3P$	500	1819	2318
23,322.66	4	$5d^7\,(^2G)\,6s\,^1G$	436	1657	2093
23,984.58	3	$5d^7(^4F)\,6s\,^3F$	−153	1572	1419
24,222.97	6	$5d^7\,(^2H)\,6s\,^3H$	716	1744	2461
24,291.97	5	$5d^6 6s^2\,^3G$	−1259	962	−297
25,069.71	2	$5d^7(^4F)\,6s\,^3F$	380	2025	2405
25,593.96	3	$5d^7\,(^2G)\,6s\,^3G$	−396	1237	841
25,601.55	4	$5d^8\,^3F$	−590	1430	840
26,200.42	4	$5d^7\,(^2G)\,6s\,^3G$	1100	2119	3219
26,416.35	6	$5d^6 6s^2\,^1I$	−2303	518	−1784
26,783.05	5	$5d^7\,(^2H)\,6s\,^3H$	525	1941	2465
27,350.96	3	$5d^6 6s^2\,^3G$	−677	1258	581
28,139.52	3	$5d^7\,(^2D)\,6s\,^3D$	−789	1328	540
28,411.95	2	$5d^7(^4P)\,6s\,^3P$	−192	1666	1473
29,394.30	4	$5d^6 6s^2\,^1G$	−457	1761	1304
30,056.79	2	$5d^8\,^3F$	141	1914	2055
31,765.12	3	$5d^8\,^3F$	261	2298	2560

[a] Gluck et al. [8].
[b] Kröger et al. [5].

Table 4
Higher-order relativistic contributions to the level specific mass shift (SMS) parameter with respect to the ground level for all known even-parity levels belonging to the $(5d+6s)^8$ configurations in Os I. $\Delta\tilde{K}^{(1)}_{SMS}$ and $\Delta\tilde{K}^{(2+3)}_{SMS}$ are respectively related to the first term and to the sum of the second and third terms of the recoil SMS Hamiltonian (see Eq. (9)). $\Delta\tilde{K}^{(1+2+3)}_{SMS}$ is the total SMS parameter.

E_{exp}[a] (cm^{-1})	J	Designation[b]	$\Delta\tilde{K}^{(1)}_{SMS}$ (GHz u)	$\Delta\tilde{K}^{(2+3)}_{SMS}$ (GHz u)	$\Delta\tilde{K}^{(1+2+3)}_{SMS}$ (GHz u)
0.00	4	$5d^6 6s^2\,^5D$	0	0	0
2740.49	2	$5d^6 6s^2\,^5D$	−239	59	−180
4159.32	3	$5d^6 6s^2\,^5D$	530	−316	215
5143.92	5	$5d^7(^4F)\,6s\,^5F$	−3832	373	−3460
5766.14	1	$5d^6 6s^2\,^5D$	536	−322	214
6092.79	0	$5d^6 6s^2\,^5D$	594	−291	304
8742.83	4	$5d^7(^4F)\,6s\,^5F$	−3389	163	−3227
10,165.98	2	$5d^6 6s^2\,^5D$	−419	−307	−727
11,030.58	4	$5d^6 6s^2\,^3G$	−510	−84	−593
11,378.00	3	$5d^7(^4F)\,6s\,^5F$	−3158	37	−3121
12,774.38	2	$5d^7(^4F)\,6s\,^5F$	−2891	−28	−2919
13,020.07	1	$5d^7(^4F)\,6s\,^5F$	−2889	15	−2874
13,364.83	2	$5d^6 6s^2\,^3F$	−506	−153	−659
14,091.37	3	$5d^6 6s^2\,^3F$	−940	−147	−1087
14,338.99	5	$5d^6 6s^2\,^3G$	−63	−191	−254
14,848.05	4	$5d^7(^4F)\,6s\,^3F$	−2170	171	−1999
14,852.33	6	$5d^6 6s^2\,^3H$	173	−242	−68
15,222.57	2	$5d^7(^4P)\,6s\,^5P$	−2160	105	−2055
15,390.76	3	$5d^7(^4P)\,6s\,^5P$	−2307	48	−2259
16,212.41	1	$5d^7(^4P)\,6s\,^5P$	−2176	−119	−2296
17,667.34	1	$5d^6 6s^2\,^3P$	−527	−311	−838
18,301.40	0	$5d^7\,(^2P)\,6s\,^3P$	486	−505	−19
18,417.12	5	$5d^7\,(^2G)\,6s\,^3G$	−1692	−132	−1824
18,901.94	3	$5d^6 6s^2\,^3D$	−1233	−110	−1343
19,048.91	0	$5d^6 6s^2\,^3P$	−1232	−92	−1323
19,108.87	4	$5d^6 6s^2\,^3G$	−1271	−208	−1479
19,410.66	2	$5d^6 6s^2\,^3D$	−323	−326	−649
19,893.07	4	$5d^6 6s^2\,^3H$	−523	−302	−826
21,033.45	1	$5d^6 6s^2\,^3D$	−1576	−194	−1769
21,123.66	3	$5d^6 6s^2\,^3G$	−412	−430	−841
21,303.36	2	$5d^6 6s^2\,^3D$	−635	−283	−917
22,563.65	1	$5d^7(^4P)\,6s\,^5P$	−391	−427	−818
23,317.60	2	$5d^7\,(^2P)\,6s\,^3P$	−1957	−128	−2084
23,322.66	4	$5d^7\,(^2G)\,6s\,^1G$	−2248	−33	−2281
23,984.58	3	$5d^7(^4F)\,6s\,^3F$	−1393	−223	−1617
24,222.97	6	$5d^7\,(^2H)\,6s\,^3H$	−2834	45	−2789
24,291.97	5	$5d^6 6s^2\,^3G$	−33	−364	−397
25,069.71	2	$5d^7(^4F)\,6s\,^3F$	−2313	−119	−2432
25,593.96	3	$5d^7\,(^2G)\,6s\,^3G$	−868	−180	−1048
25,601.55	4	$5d^8\,^3F$	−1039	−274	−1313
26,200.42	4	$5d^7\,(^2G)\,6s\,^3G$	−3314	76	−3238
26,416.35	6	$5d^6 6s^2\,^1I$	874	−587	288
26,783.05	5	$5d^7\,(^2H)\,6s\,^3H$	−2794	−33	−2827
27,350.96	3	$5d^6 6s^2\,^3G$	−355	−212	−567
28,139.52	3	$5d^7\,(^2D)\,6s\,^3D$	−636	−313	−949
28,411.95	2	$5d^7(^4P)\,6s\,^3P$	−1205	−132	−1337
29,394.30	4	$5d^6 6s^2\,^1G$	−1474	−272	−1746
30,056.79	2	$5d^8\,^3F$	−1938	−106	−2044
31,765.12	3	$5d^8\,^3F$	−2531	−149	−2680

[a] Gluck et al. [8].
[b] Kröger et al. [5].

them, they used the scaling law for the NMS [5] which we have just shown it is no more valid for Os I. In Table 5, we compare therefore the experimental values of Kröger et al. [5] corrected with the scaling law they used to retrieve the total experimental IS, $\delta\nu^{Tot}_{Expt}$, for the even-parity levels with our MCDHF total isotope shifts, $\delta\nu^{Tot}_{MCDHF}$. Our MCDHF normal mass shift, $\delta\nu^{NMS}_{MCDHF}$, specific mass shift, $\delta\nu^{SMS}_{MCDHF}$ and the field shift, $\delta\nu^{FS}_{MCDHF}$, are also given. These values are calculated using the root-mean-square nuclear charge radii tabulated by Angeli and Marinova [24], i.e. $\delta\langle r^2\rangle^{192,190} = \langle r^2\rangle^{192} - \langle r^2\rangle^{190} = 0.068\ \mathrm{fm}^2$, and the nuclear masses obtained by the RIS3 code from the atomic mass numbers. First, one can notice the dominance of the field

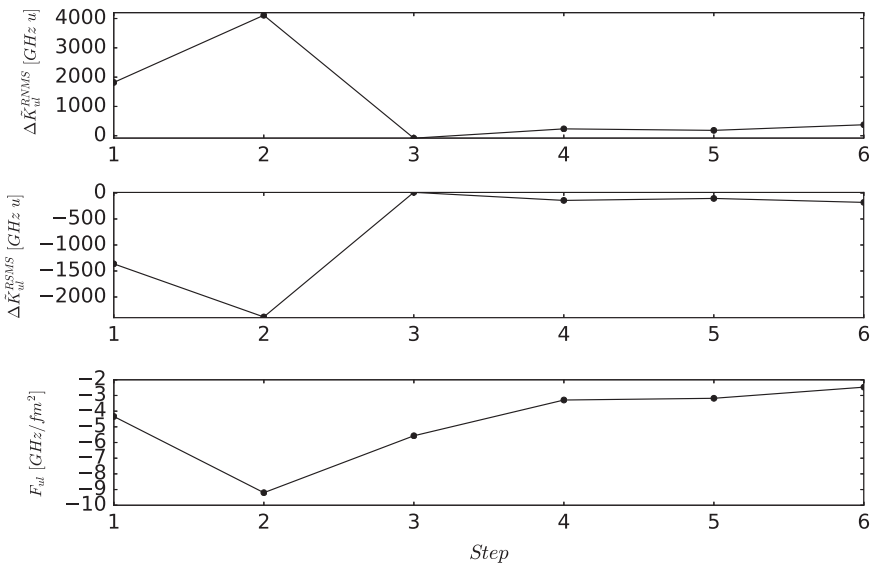

Fig. 1. Transition isotope shift electronic parameters, i.e. the normal mass shift parameter $\Delta\tilde{K}_{ul}^{RNMS}$, the specific mass shift parameter $\Delta\tilde{K}_{ul}^{RSMS}$ and the field-shift factor F_{ul}, for the transition $5d^56s^2\ ^5D_4$–$5d^56s^2\ ^5D_2$ in Os I as a function of the MCDHF calculation step. For each parameter, a reasonable convergence has been achieved in the last three steps.

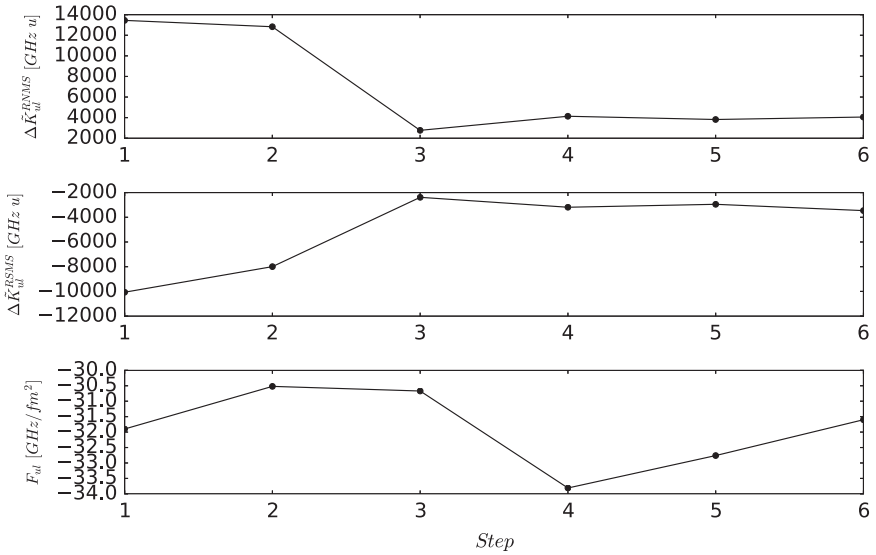

Fig. 2. Transition isotope shift electronic parameters, i.e. the normal mass shift parameter $\Delta\tilde{K}_{ul}^{RNMS}$, the specific mass shift parameter $\Delta\tilde{K}_{ul}^{RSMS}$ and the field-shift factor F_{ul}, for the transition $5d^56s^2\ ^5D_4$–$5d^66s\ ^5F_5$ in Os I as a function of the MCDHF calculation step. For the *RMS* parameters, a reasonable convergence has been achieved in the last three steps. The FS factor is relatively stable along the steps, the y-scale indicating a variation of 4 GHz/fm^2 (i.e. $\sim$10%).

shift contributions over the normal and specific mass shifts with the remarkable exceptions of the levels $5d^66s^2\ ^5D_{1,3}$,$^3H_6$. For the latter level, the field shift is almost cancelled by the normal mass shift. Finally, the comparison between the experimental and MCDHF total isotope shifts shows a good agreement for most of the levels given the experimental error bars and the complexity of the atomic structure. In that regard, the experimental error bar concerning level $5d^8\ ^3F_4$ is particularly large and, in that case, a more precise measurement is needed for constraining our model.

4. Conclusions

The electronic isotope shift parameters, i.e. the normal mass shift, specific mass shift and field shift electronic parameters, have been calculated for all the fine-structure

Table 5
MCDHF level isotope shifts (IS), $\delta\nu_{MCDHF}$, for the even-parity levels of ^{192}Os I and comparison with experiment. All IS values are given with respect to the ground state and to the ^{190}Os isotope.

Energy[a] (cm^{-1})	Level[b]	$\delta\nu^{NMS}_{MCDHF}$ (MHz)	$\delta\nu^{SMS}_{MCDHF}$ (MHz)	$\delta\nu^{FS}_{MCDHF}$ (MHz)	$\delta\nu^{Tot}_{MCDHF}$ (MHz)	$\delta\nu^{Tot(b)}_{Expt}$ (MHz)
0.00	$5d^6\ 6s^2\ ^5D_4$	0	0	0	0	0
2740.49	$5d^6\ 6s^2\ ^5D_2$	−21	10	−168	−179	−167(90)
4159.32	$5d^6\ 6s^2\ ^5D_3$	30	−12	31	49	34(80)
5143.92	$5d^7\ 6s\ ^5F_5$	−223	190	−2149	−2182	−2235(60)
5766.14	$5d^6\ 6s^2\ ^5D_1$	28	−12	−13	3	−61(80)
8742.83	$5d^7\ 6s\ ^5F_4$	−196	177	−2111	−2130	−2117(80)
11,030.58	$5d^6\ 6s^2\ ^3F_4$	−20	33	−501	−488	−416(5)
11,378.00	$5d^7\ 6s\ ^5F_3$	−186	171	−2126	−2141	−2129(60)
12,774.38	$5d^7\ 6s\ ^5F_2$	−171	160	−2045	−2056	−1905(70)
13,020.07	$5d^7 6s\ ^5F_1$	−172	158	−2037	−2051	−2122(80)
13,364.83	$5d^7\ 6s\ ^3F_2$	−29	36	−603	−596	−687(70)
14,091.37	$5d^6\ 6s^2\ ^3F_3$	−51	60	−900	−891	−776(90)
14,338.99	$5d^6\ 6s^2\ ^3G_5$	17	14	−259	−228	−105(80)
14,848.05	$5d^7\ 6s\ ^3F_4$	−109	110	−1478	−1477	−1669(60)
14,852.33	$5d^6\ 6s^2\ ^3H_6$	45	4	−46	3	7(90)
15,222.57	$5d^7\ 6s\ ^5P_2$	−140	113	−1704	−1731	−1655(70)
15,390.76	$5d^7\ 6s\ ^5P_3$	−147	124	−1796	−1819	−1902(70)
16,212.41	$5d^7\ 6s\ ^5P_1$	−140	126	−1788	−1802	−2040(80)
17,667.34	$5d^6\ 6s^2\ ^3P_1$	−39	46	−931	−924	−755(90)
18,301.40	$5d^6\ 6s^2\ ^3P_0$	15	1	−478	−462	−491(100)
18,901.94	$5d^6\ 6s^2\ ^3D_3$	−75	74	−1274	−1275	−1174(80)
21,033.45	$5d^6\ 6s^2\ ^3D_1$	−103	97	−1638	−1644	−1240(90)
21,123.66	$5d^6\ 6s^2\ ^3G_3$	−15	46	−842	−811	−619(80)
21,303.36	$5d^6\ 6s^2\ ^3D_2$	−46	50	−1063	−1059	−1047(70)
22,563.65	$5d^7\ 6s\ ^3P_1$	−36	45	−1048	−1039	−1227(90)
23,317.60	$5d^7\ 6s\ ^3P_2$	−127	114	−1930	−1943	−1877(80)
23,322.66	$5d^7\ 6s\ ^1G_4$	−115	125	−1836	−1826	−2057(80)
25,601.55	$5d^8\ ^3F_4$	−46	72	−1353	−1327	−2532(1000)

[a] Gluck et al. [8].
[b] Kröger et al. [5]. The residual isotope shifts have been corrected using the scaling law to recover the total shifts.

levels of the even configurations $(5d+6s)^8$ of neutral osmium, Os I using the fully relativistic MCDHF method. These values can be used to determine the line and level shifts for any pair of neutral osmium isotopes. Comparison with the experimental fine-structure level shifts by Kröger et al. [5] for the isotope pair ^{190,192}Os I shows a good agreement with our MCDHF predictions.

Acknowledgements

PP and PQ are, respectively, Research Associate and Research Director of the Belgian Fund for Scientific Research F.R.S.-FNRS. Financial support from this organisation is gratefully acknowledged (Grant nos. FC 49142 and FC 37552). This work has been funded by the Interuniversity Attraction Poles Programme initiated by the Belgian Policy Office (BriX network P7/12).

References

[1] Murakawa K, Suwa S. Hyperfine structure in the spectra of iridium and osmium. Phys Rev 1957;87:1048.
[2] Guthöhrlein GH, Kopferman H, Nöldeke G, Steudel AZ. The nuclear moments and the relative isotope shift of ^{187}Os. Z Phys 1961;165:356.
[3] Hines AP, Ross JS. Isotope shift in the spectrum of osmium. Phys Rev 1962;126:2105.
[4] Aufmuth P, Wöbkler E. Isotope shift in osmium: I experiment and theory. Z Phys A 1985;321:65.
[5] Kröger S, Basar G, Baier A, Guthöhrlein GH. Hyperfine structure and isotope shift of osmium I. Phys Scr 2002;65:56.
[6] Mahgoub M. Isotope shifts of stable osmium and tungsten isotopes, MSc dissertation. University of Manchester; 2002.
[7] Avgoulea M, Mahgoub M, Billowes J, Campbell P, Ezwam A, Forest DH, et al. Laser spectroscopy of stable os isotopes. Hyperfine Interact 2006;171:217.
[8] Gluck G, Bordarier Y, Bauche J, van Kleef ThAM. Déplacement isotopique, calculs théoriques et structure de termes dans le spectre d'arc de l'osmium. Physica 1964;30:2068.
[9] Bauche J. Etude paramétrique du déplacement isotopique. Physica 1969;44:291.
[10] van Kleef TAM, Klinkenberg PFA. Spectral structure of neutral and ionized osmium. Physica 1961;27:83.
[11] Bouazza S, Guern Y, Bauche J. Isotope shift and hyperfine structure in low-lying levels of pb II. J Phys B 1986;19:1881.
[12] Jönsson P, Gaigalas G, Bieroń J, Froese Fischer C, Grant IP. New version: GRASP2K relativistic atomic structure package. Comput Phys Commun 2013;184:2197–203.
[13] Nazé C, Gaidamauskas E, Gaigalas G, Godefroid M, Jönsson P. RIS3: a program for relativistic isotopic shift calculations. Comput Phys Commun 2013;183:2187–96.
[14] Shabaev MV. Mass correction in a strong nuclear field. Theor Math Phys 1985;63:588–96.
[15] Shabaev MV. QED theory of the nuclear recoil effect in atoms. Phys Rev A 1998;57:59–67.
[16] Palmer CWP. Reformulation of the theory of the mass shift. J Phys B 1987;20:5987–96.
[17] Grant IP. In: Wilson S, editor, Methods of computational chemistry, vol. 2. New York: Plenum Press; 1988. p. 1.

[18] Parpia FA, Mohanty AK. Relativistic basis-set calculations for atoms with fermi nuclei. Phys Rev A 1992;46:3735–45.
[19] Olsen J, Roos BO, Jørgensen P, Jensen HJA. Determinant based configuration interaction algorithms for complete and restricted configuration interaction spaces. J Chem Phys 1988;89:2185–92.
[20] Coursey JS, Schwab DJ, Tsai JJ, Dragoset RA. Atomic weights and isotopic compositions (version 3.0). National Institute of Standards and Technology, Gaithersburg, MD. ⟨http://physics.nist.gov/pml/data/comp.cfm⟩ [last 18.12.15].
[21] Li JG, Nazé C, Godefroid MR, Gaigalas Jönsson P. On the breakdown of the Dirac kinetic energy operator for estimating normal mass shifts. Eur Phys J D 2012;66:290.
[22] Veitia A, Pachucki K. Nuclear recoil effects in antiprotonic and muonic atoms. Phys Rev A 2004;69:042501.
[23] Kozlov MG, Korol VA. Relativistic and correlation corrections to the isotope shift in Ba II and Ba I. Unpublished work.
[24] Angeli I, Marinova KP. Table of experimental nuclear ground state charge radii: an update. Data Nucl Data Tables 99 2013;69:95.